76295

Impact Melt Breccia

260.7 grams

Figure 1: Astronaut pushing rover uphill. Broken boulder at station 6, Apollo 17. Boulder tracks lead back up North Massif. NASA# AS-17-164-5954.

Figure 2: Fresh broken surface of 76295, chipped off of block 1 of large boulder in figure 1. Scale is 1 cm. NASA# S72-56409.

Introduction

Sample 76295 was chipped from block 1 of the big boulder at station 6 (figure 1; Wolfe et al. 1981; Heiken et al. 1973; Meyer 1994). Tracks made by this broken boulder show that it originated high up on the North Massif. The interpretation is that this boulder was part of the ejecta blanket from the gigantic impact that produced the Serenitatis Basin.

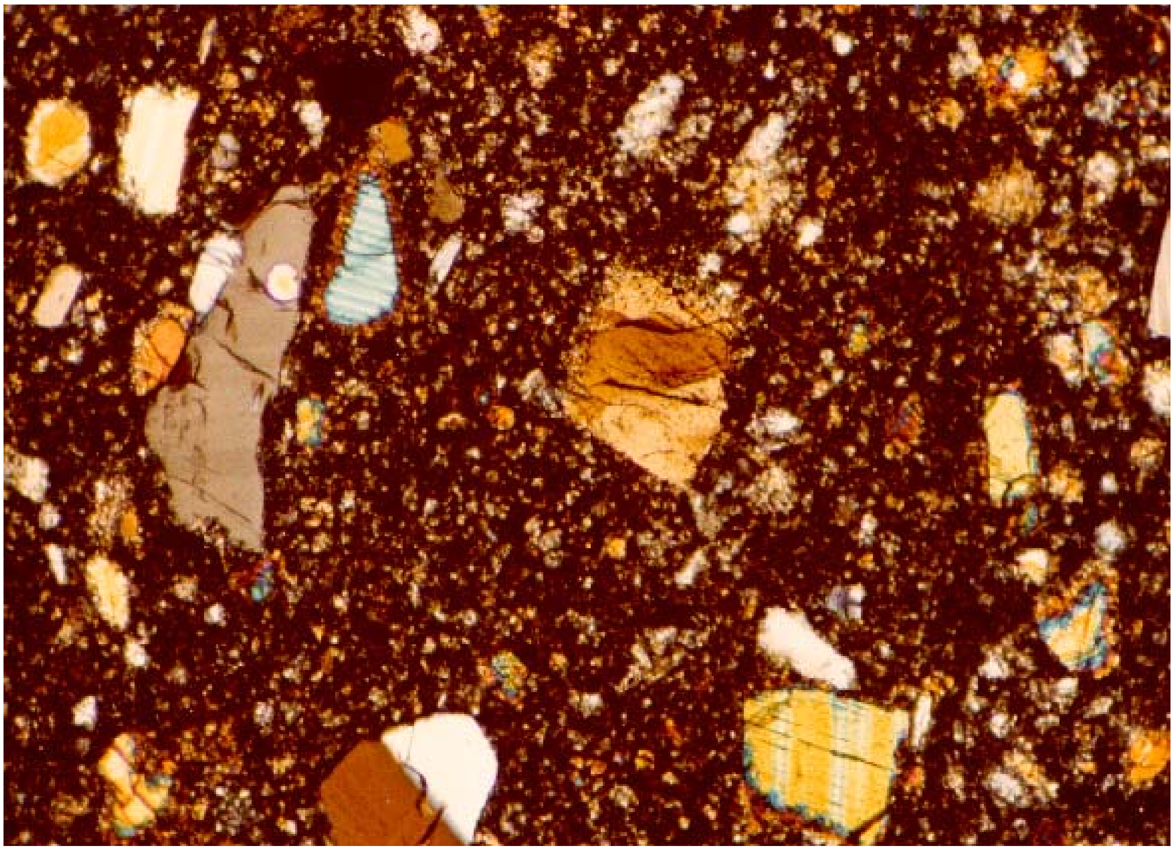

Figure 3: Photomicrograph of thin section (crosssed Nicols) illustrating mineral clasts in matrix of of 76295. Scale: field of view is 1.4 mm. NASA# S79-27273

This important boulder was observed to be made of three lithologic units (76295 is from unit C). 76295 is a non-vesicular, crystalline matrix breccia with a blue-grey color (similar to 76275). Light and dark clasts have a distinct outline with the matrix (figure 2). The B1 surface has zap pits, while the N1 surface is freshly broken. The other surfaces of the rock were covered with a "buff powder" and/or "patina" (Heiken et al. 1973).

The fine grain texture and overall clast/matrix texture of 76295 and 76275 were important evidence for the thermal model developed by Simonds (1975) and Onorato et al. (1976) for the genesis of impact melt breccias. Briefly, this model is that hot impact melt entrained, and was quickly cooled, by cold clastic debris that was partially digested. The resulting melt sheet then crystallized to a fine grain matrix including undigested mineral and lithic clasts.

Petrography

Sample 76295 has been described by Heiken et al. (1973) and Simonds (1975) as a fine subophitic impact melt. It is a banded, clast-bearing, nonvesicular, blue-grey breccia with aphanitic matrix. The blue-grey breccia matrix contains bands and swirls of minor (~10%) tan matrix breccia and partially dissolved mineral and rock clasts. A slab sawn from the breccia (,12) and the other saw cuts illustrates the "marbled" texture of the tan and blue-grey breccia matrix (figure 11). Four individual rock clasts have been studied by Simonds (1975, McGee et al. 1977).

Significant Clasts

Dark grey: Subophitic melt rock similar to matrix. Table 1, figure 8.
Light grey: Poikilitic melt rock similar to 76015. Table 1, figure 8.
Porous Basalt Clast: Similar to a basalt clast in 76015. Simonds (1975) Table 1, figures 5, 8.
Troctolite Clast (feldpathic olivine norite): Monomict breccia. Simonds (1975), Phinney (1981) Figure 6.

The matrix of 76295 is holocrystalline with only minor void space. The mode is about 50% plagioclase and 40% pyroxene with minor ilmenite, olivine and other

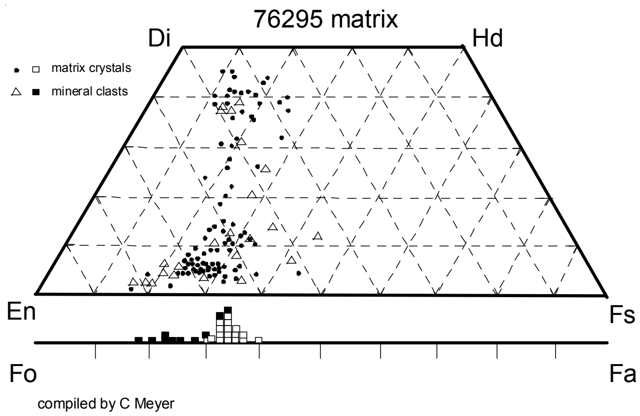

Figure 4: Composition of pyroxene and olivine in matrix of 76295 (data replotted from Phinney 1981).

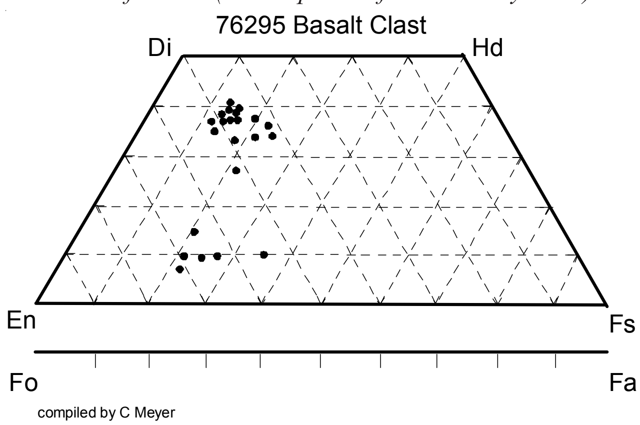

Figure 5: Composition of pyroxene and olivine in basalt clast within 76295 (data replotted from Phinney 1981).

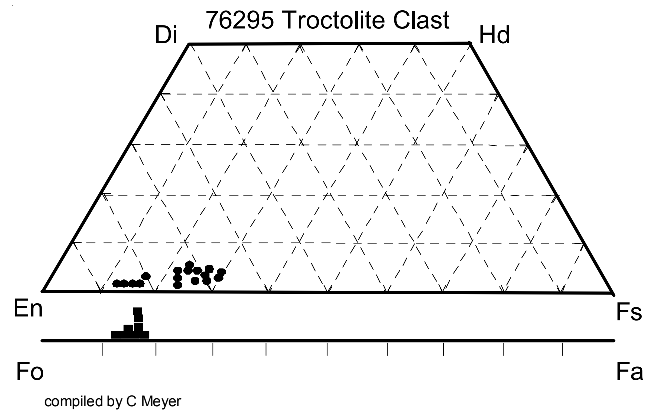

Figure 6: Composition of pyroxene and olivine in troctolite clast of 76295 (data replotted from Phinney 1981).

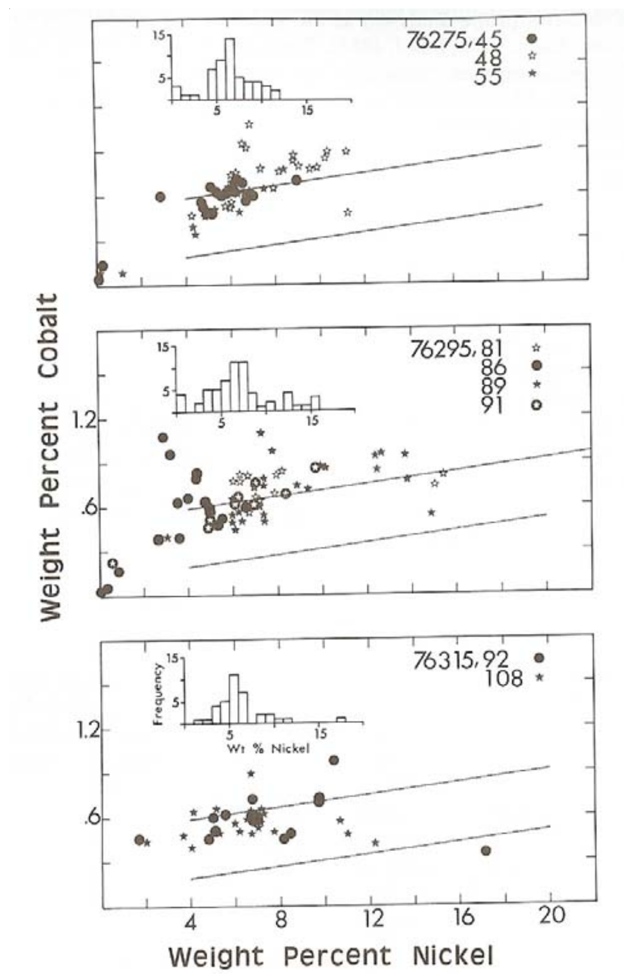

Figure 7: Ni and Co content of metal grains in 76295 (Misra et al. 1976).

minerals. Grain size of matrix feldspar is <15 microns, pyroxene 10-25 microns.

Norman et al. (1993) have compared the compositions of minerals in LKFM clasts in 76295 with minerals in similar clasts in 76315 and conclude that the clast population in 76295 is dominated by "Mg-suite norites, troctolites and gabbronorites". Minor-element abundances in both olivine and pyroxene are unlike those found in lunar rocks of the ferroan anorthosite suite.

Mineralogical mode for 76295

	Matrix	Basalt clast	Troctolitic clast
Plagioclase	50 %	50	50
Pigeonite	34	10	32
Augite	7	30	1
Olivine	7	0	17
Ilmenite	1	10	1

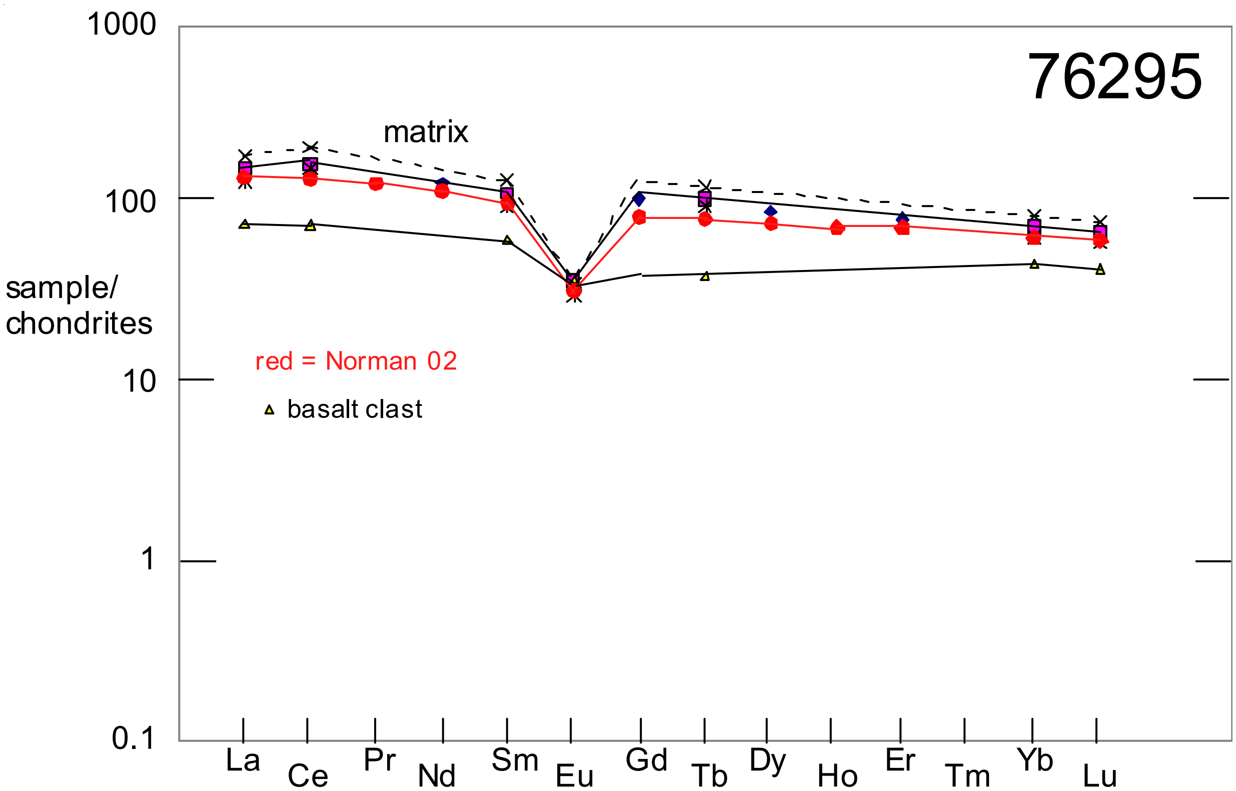

Figure 8: Normalized rare-earth-element composition diagram for matrix and clasts in 76295 (see table 1 for source of data).

Mineralogy

Olivine: Olivine is generally Fo_{67-78} (Norman et al. 1993; Simonds 1975).

Pyroxene: The composition of pyroxene and olivine is shown in figure 4 – 6.

Plagioclase: Plagioclase is generally in the range of An_{81-97} (Norman et al. 1993).

Zircon: Meyer found one large rounded zircon in the matrix of 76295 (figure 9).

Metal: Misra et al. (1976) studied the nickel-iron particles in 76295 (figure 7).

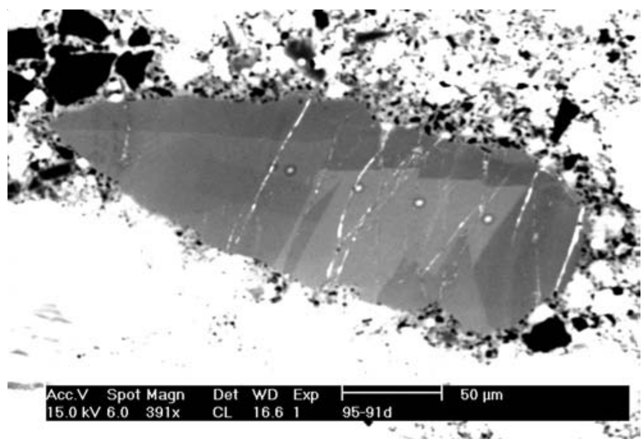

Figure 9: Back scattered electron image of large zircon grain in 76295 - called "arrowhead" by Pidgeon et al. 2006.

Chemistry

The chemical composition of the blue-grey and tan matrix portions of 76295 were found to be identical (table 1; figure 8). Unpublished data can be found in Simonds and Warner (1981) and Phinney (1981). Higuchi and Morgan (1975) found that the matrix samples of 76295 were tightly grouped within meteorite group 2 on an Ir-Au-Re diagram, but that clasts extracted from 76295 had different ratios (figure 10).

The composition determined for the porous basalt clast was "unusual".

Note: There appears to a mistake in the tabulation of data from Higuchi and Morgan (1975) for 76295 matrix in Simonds (1975).

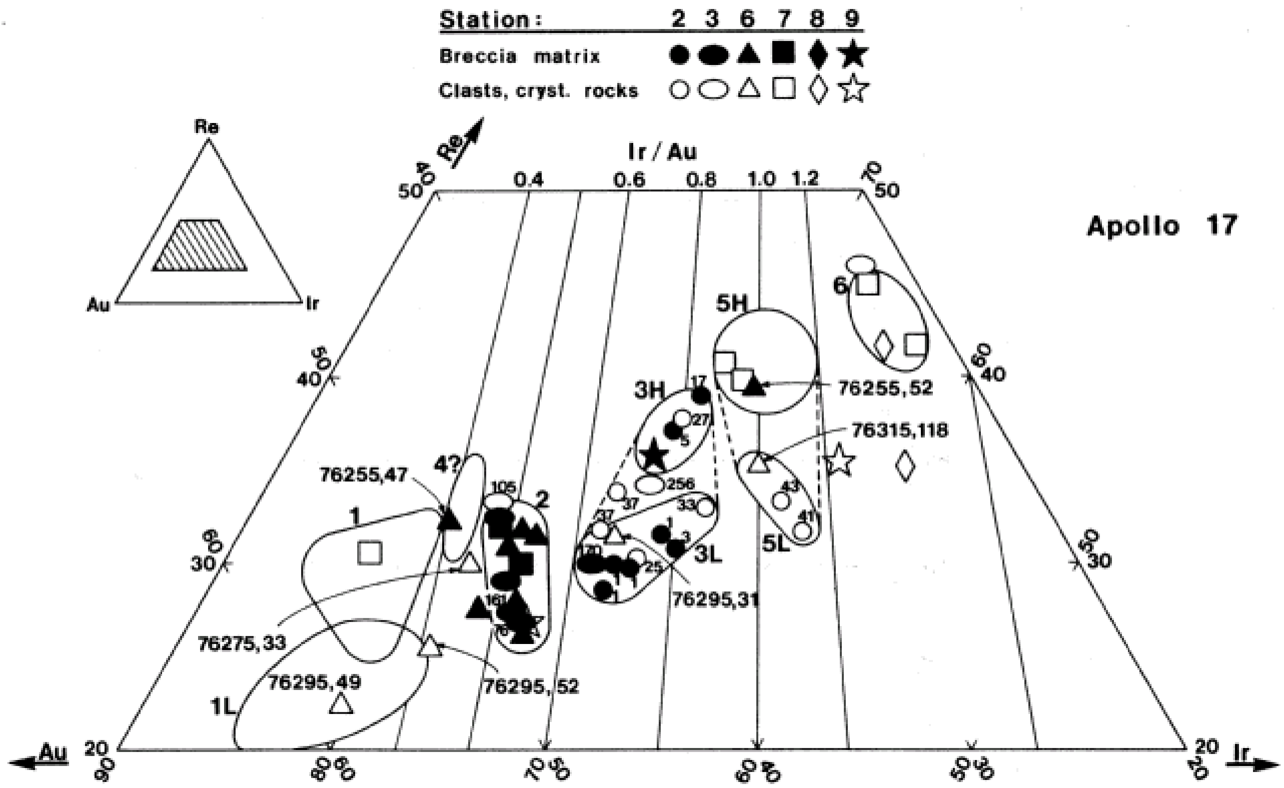

Figure 10: Composition diagram for three trace elements (Ir, Au and Re) showing tight grouping for matrix, but dispersed grouping for clasts in 76295 (figure from Higuchi and Morgan 1975).

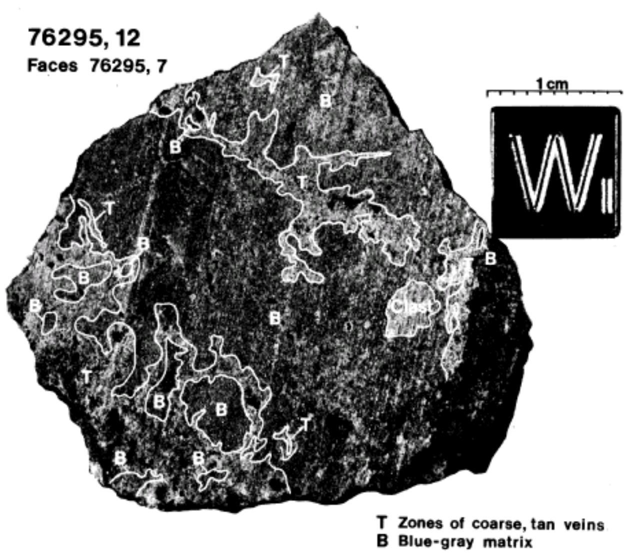

Figure 11: Map of slab through 76295 showing marbled texture of blue-grey and tan matrix (from Phinney et al. 1981).

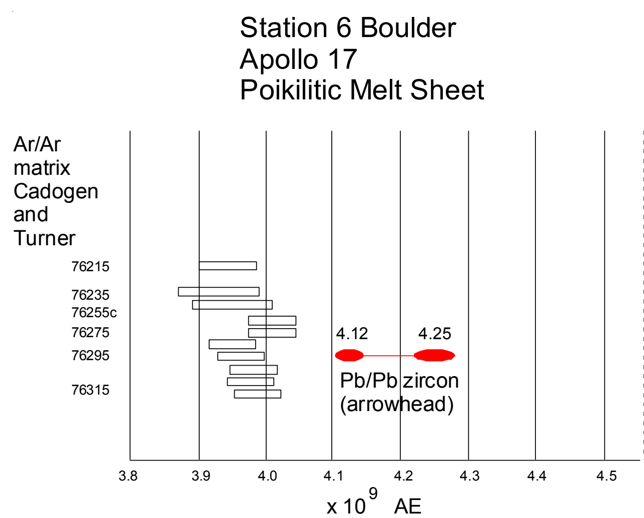

Figure 12: Summary diagram for ages of 76295

Radiogenic age dating

Cadogan and Turner (1976) determined the crystallization age of two samples of 76295 by the ^{39}Ar-^{40}Ar plateau technique. The tan matrix yielded an intermediate temperature plateau age of 3.95 ± 0.04 b.y., and the blue grey matrix yielded and age of 3.96 ± 0.04 b.y. However, both sub-samples exhibited

Table 1a. Chemical composition of 76295.

reference	Simonds 75	Higuchi 75	Phinney 81	Higuchi 75	Phinney 81	Higuchi 75	Wiesmann 75	Phinney 81	Phinney 81
weight	blue matrix	blue matrix	tan matrix	tan matrix	basalt clast	basalt clast	basalt clast	dark grey	light grey
SiO_2 %	47.03 (a)		*47.55* (d)		*48.11* (d)			*46.89*	*47.04*
TiO_2	1.39 (a)		*1.64* (d)		*1.8* (d)		1.85 (b)	*1.5*	*1.36*
Al_2O_3	18.25 (a)		*17.67* (d)		*16.95* (d)			*18.67*	*18.98*
FeO	9.09 (a)		*9.05* (d)		*9.17* (d)			*8.79*	*8.44*
MnO									
MgO	10.78 (a)		*9.78* (d)		*9.72* (d)			*9.66*	*9.64*
CaO	11.54 (a)		*11.49* (d)		*11.22* (d)			*11.69*	*11.95*
Na_2O	0.76 (a)		*0.74* (d)		*0.75* (d)			*0.71*	*0.66*
K_2O	0.26 (a)		*0.29* (d)		*0.6* (d)			*0.23*	*0.28*
P_2O_5	0.32 (a)								
S %	0.06 (a)								
sum									
Sc ppm			17.8 (e)		21 (e)			18.2	16.7
V									
Cr			1382 (e)		1440 (e)		1364 (b)	1440	1360
Co			19.9 (e)		24.9 (e)			28	23.1
Ni		250 (c)	160 (e)	218 (c)	230 (e)	146 (c)		203	179
Cu									
Zn		27.1 (c)	20 (e)	2.5 (c)		2.2 (c)		2.6	2.3
Ga									
Ge ppb		316 (c)		374 (c)		321 (c)		423	198
As									
Se		103 (c)		132 (c)		235 (c)		68	75
Rb	5.43 (b)	9.2 (c)		4.22 (c)		12.5 (c)	20.47 (b)	1.75	3.31
Sr	175 (b)						191 (b)		
Y									
Zr	541 (b)						232 (b)		
Nb									
Mo									
Ru									
Rh									
Pd ppb									
Ag ppb		4.55 (c)		5.09 (c)		1.03 (c)		1.2	0.87
Cd ppb		6.56 (c)		1 (c)		1.13 (c)		1.28	1.88
In ppb									
Sn ppb									
Sb ppb		393 (c)		1.68 (c)		1.84 (c)		2.11	1.03
Te ppb		4.9 (c)		4.62 (c)		5.81 (c)		1.9	2.4
Cs ppm		0.151 (c)		0.297 (c)		0.649 (c)		0.11	0.192
Ba	376 (b)						334 (b)		
La	37.8 (b)		37.5 (e)		22 (e)		18.2 (b)	44.2	31.8
Ce	95.7 (b)		102 (e)		59 (e)		46.6 (b)	127	95.8
Pr									
Nd	60 (b)						31.1 (b)		
Sm	16.9 (b)		17 (e)		10.9 (e)		9.22 (b)	20.4	14.3
Eu	1.91 (b)		2.11 (e)		2.15 (e)		2.08 (b)	2.01	1.77
Gd	21.3 (b)						12.4 (b)		
Tb			3.91 (e)		2.72 (e)			4.56	3.56
Dy	22.3 (b)						13.3 (b)		
Ho									
Er	13.2 (b)						8.06 (b)		
Tm									
Yb	12 (b)		12.2 (e)		8.8 (e)		7.6 (b)	14.1	10.8
Lu			1.71 (e)		1.31 (e)		1.07 (b)	1.95	1.49
Hf			13.2 (e)		7.9 (e)			16.3	12.4
Ta			1.9 (e)		1.4 (e)			2.4	1.7
W ppb									
Re ppb		0.566 (c)		0.486 (c)		0.267 (c)		0.456	0.48
Os ppb									
Ir ppb		7.88 (c)		6.1 (c)		3.18 (c)		5.42	5.98
Pt ppb									
Au ppb		4.36 (c)		3.43 (c)		2.91 (c)		3.93	2.65
Th ppm	6.12 (b)		5.6 (e)		2.2 (e)		2.01 (b)	7.6	5.2
U ppm	1.83 (b)	1.9 (c)		1.32 (c)		0.76 (c)	0.66 (b)	1.94	1.62

technique (a) XRF, (b) IDMS, (c) RNAA, (d) fused bead, (e) INAA

Table 2. Light and/or volatile elements for 76295.

reference	Simonds 75	Higuchi 75	Phinney 81	Higuchi 75	Phinney 81	Higuchi 75	Wiesmann 75	Phinney 81	Phinney 81
weight	blue matrix	blue matrix	tan matrix	tan matrix	basalt clast	basalt clast	basalt clast	dark grey	light grey
Li ppm	19.4 (b)						20.5 (b)		
Be									
B		Phinney 1981							
C		105							
S		731							
F ppm									
Cl									
Br ppb		78.7 (c)		27.9 (c)		30.5 (c)		37.5	23.5
I									
Pb ppm									
Hg ppb									
Tl		1.41 (c)		0.64 (c)		0.99 (c)		0.33	0.44
Bi		0.97 (c)		0.8 (c)		0.4 (c)		0.56	0.46

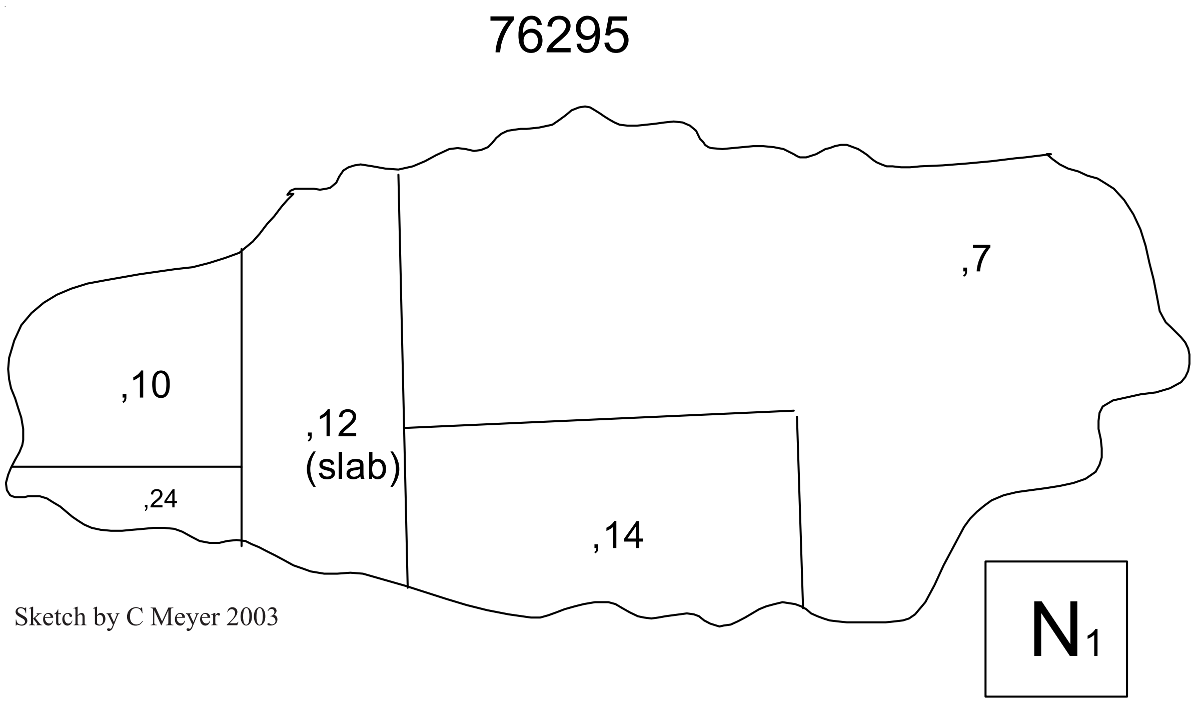

Figure 13: Initial saw cuts of 76295 (campare with figure 2).

Table 3: Radiation Counting for 76295.

	Oak Ridge	Battelle
Th ppm	5.4	5.76
U ppm	1.5	1.55
K %	0.227	0.23
26Al	67 dpm/kg	71
22Na	54	64
54Mn	38	70
56Co	41	35
46Sc	5	6.4
48V		
69Co		< 1.2

as reported in Heiken et al. 1973

appreciable decreases in ^{40}Ar over the last 30% high-temperature release (figure 14).

Unpublished elemental and isotopic data for U, Th and Pb by Leon Silver and Rb-Sr by Larry Nyquist were reported in Phinney (1981).

A large zircon in 76295 has been dated at ~4.25 b.y. (with 4.12 b.y. overgrowth) by the ion probe method (Pidgeon et al. 2006; Nemchin et al. 2010) (figures 9 and 12).

Table 1b. Chemical composition of 76295.

reference	Norman 02		Eldridge74	Ramcitelli74	
weight	3 g				
SiO2 %	46.4	(b)			
TiO2	1.49	(b)			
Al2O3	18.2	(b)			
FeO	8.39	(b)			
MnO	0.12	(b)			
MgO	10.5	(b)			
CaO	11.2	(b)			
Na2O	0.71	(b)			
K2O	0.34	(b)	0.273	0.28	(c)
P2O5					
S %					
sum					
Sc ppm	18.4	(a)			
V	45	(a)			
Cr	1325	(a)			
Co	26.4	(a)			
Ni	208	(a)			
Cu	11.6	(a)			
Zn	14	(a)			
Ga	5.3	(a)			
Ge ppb					
As					
Se					
Rb	7.5	(a)			
Sr	183	(a)			
Y	132	(a)			
Zr	587	(a)			
Nb	37.7	(a)			
Mo					
Ru ppb	10.5	(c)			
Rh					
Pd ppb	11	(c)			
Ag ppb					
Cd ppb					
In ppb					
Sn ppb					
Sb ppb					
Te ppb					
Cs ppm	0.29	(a)			
Ba	378	(a)			
La	33.3	(a)			
Ce	84.7	(a)			
Pr	11.7	(a)			
Nd	53.8	(a)			
Sm	15.2	(a)			
Eu	1.85	(a)			
Gd	16.8	(a)			
Tb	3	(a)			
Dy	19	(a)			
Ho	4.1	(a)			
Er	11.7	(a)			
Tm					
Yb	10.5	(a)			
Lu	1.53	(a)			
Hf	11.8	(a)			
Ta	1.6	(a)			
W ppb	920	(a)			
Re ppb	0.56	(c)			
Os ppb					
Ir ppb	5.61	(c)			
Pt ppb	12.3	(c)			
Au ppb					
Th ppm	6.41	(a)	5.3	5.76	(c)
U ppm	1.64	(a)	1.5	1.55	(c)

technique: (a) ICP-MS, (c) radiation counting

Cosmogenic isotopes and exposure ages

Data from radiation counting is given in Heiken et al. (1973) (table 3). Unpublished isotopic data for He, Ne, Ar, Kr and Xe by as determined by Bogard are found in Phinney (1981).

O'Kelley et al. (1974) determined the cosmic-ray-induced activity of ^{26}Al = 67 dpm/kg., ^{22}Na = 54 dpm/kg, ^{54}Mn = 38 dpm/kg, ^{56}Co = 41 dpm/kg. and ^{46}Sc = 5 dpm/kg. Rancitelli et al. (1974) determined ^{26}Al = 71 dpm/kg, ^{22}Na = 64 dpm/kg, ^{54}Mn = 69 dpm/kg, ^{56}Co =35 dpm/kg,

Other Studies

Gose et al. (1978) propose that the large scatter of magnetization direction of 76295 implies the predominance of pre-impact magnetization in this sample. Brecher (1976) makes convincing argument that alignment of magnetization follows the direction of foliation and is caused by "textural remanent magnetization".

Processing

Sample 76295 was one of the samples studied by the Station 6 Boulder Consortium led by Bill Phinney. A detailed guidebook of the results of this consortium is available from the Curator (Phinney 1981). Lithological maps of the boulders and of the samples are presented in a Tech Report by Heiken et al. (1973). The sketch in figure 13 shows the approximate location of the saw cuts for initial processing of 76295. The map of slab (,12) reproduced in figure 11 shows the tan lithology is surrounded by the more abundant blue-grey lithology.

There are 19 thin sections.

List of Photos

S72-56406-56411 PET mug shots
S74-18439-18446 saw cuts
S74-20186-20190 group photos
S74-20819
S77-26955
S79-27270-27274 thin section photos

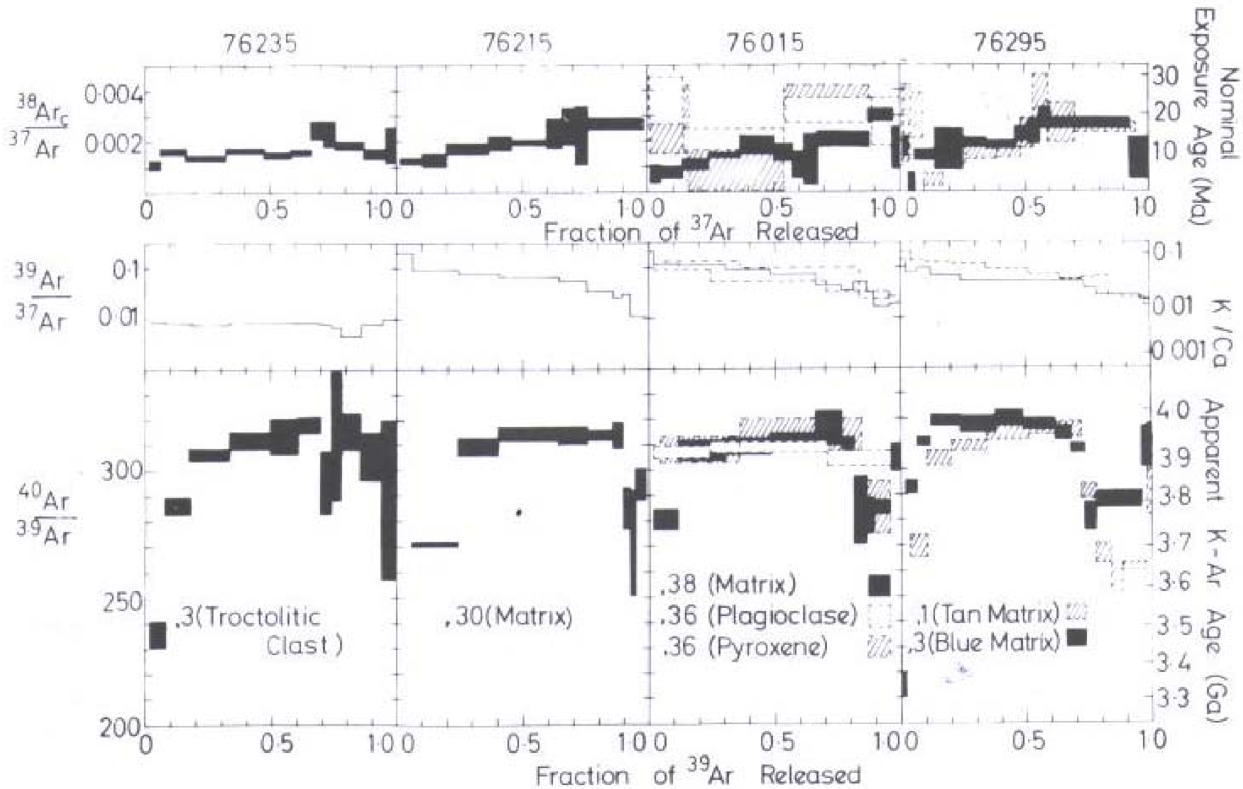

Figure 14: Ar39-40 release diagram for samples from station 6 boulder compared with with two matrix samples of 76295 (from Cadogan and Turner 1976).

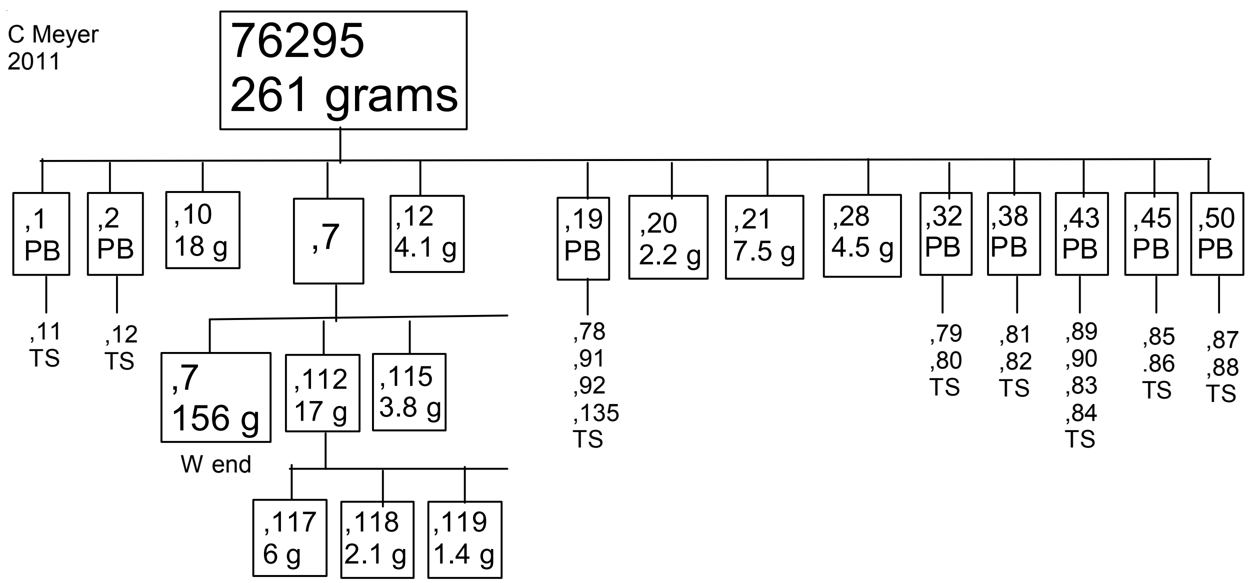

References for 76295

Brecher A. (1976a) Textural remanence: A new model of lunar rock magnetism. *Earth Planet. Sci. Lett.* **29**, 131-145.

Butler P. (1973) **Lunar Sample Information Catalog Apollo 17.** Lunar Receiving Laboratory. MSC 03211 Curator's Catalog. pp. 447.

Cadogan P.H. and Turner G. (1976) The chronology of the Apollo 17 Station 6 boulder. *Proc. 7th Lunar Sci. Conf.* 2267-2285.

Eldridge J.S., O'Kelley G.D. and Northcutt K.J. (1974a) Primordial radioelement concentrations in rocks and soils from Taurus-Littrow. *Proc. 5th Lunar Sci. Conf.* 1025-1033.

Gose W.A., Strangway D.W. and Pearce G.W. (1978) Origin of magnetization in lunar breccias: An example of thermal overprinting. *Earth Planet. Sci. Lett.* **38**, 373-384.

Heiken G.H., Butler P., Simonds C.H., Phinney W.C., Warner J., Schmitt H.H., Bogard D.D. and Pearce W.G. (1973a) Preliminary data on boulders at Station 6, Apollo 17 landing site. NASA TMX-58116, pp. 56.

Higuchi H. and Morgan J.W. (1975a) Ancient meteoritic component in Apollo 17 boulders. *Proc. 6th Lunar Sci. Conf.* 1625-1651.

Hertogen J., Janssens M.-J., Takahashi H., Palme H. and Anders E. (1977) Lunar basins and craters: Evidence for systematic compositional changes of bombarding population. *Proc. 8th Lunar Sci. Conf.* 17-45.

LSPET (1973) Apollo 17 lunar samples: Chemical and petrographic description. *Science* **182**, 659-672.

LSPET (1973) Preliminary Examination of lunar samples. Apollo 17 Preliminary Science Rpt. NASA SP-330. 7-1 – 7-46.

Misra K.C., Walker B.M. and Taylor L.A. (1976a) Textures and compositions of metal particles in Apollo 17, Station 6 boulder samples. *Proc. 7th Lunar Sci. Conf.* 2251-2266.

Misra K.C., Walker B.M. and Taylor L.A. (1976b) Native FeNi metal particles in Apollo 17 Station 6 boulder (abs). *Lunar Sci.* **VII**, 565-567. Lunar Planetary Institute, Houston.

McGee P.E., Simonds C.H., Warner J.L. and Phinney W.C. (1979) Introduction to the Apollo Collections: Part II Lunar Breccias. Curators Office.

Meyer C. (1994) Catalog of Apollo 17 rocks. Vol. 4 North Massif

Muehlberger et al. (1973) Documentation and environment of the Apollo 17 samples: A preliminary report. Astrogeology 71 322 pp superceeded by Astrogeology 73 (1975) and by Wolfe et al. (1981)

Muehlberger W.R. and many others (1973) Preliminary Geological Investigation of the Apollo 17 Landing Site. *In* **Apollo 17 Preliminary Science Report.** NASA SP-330.

Nemchin A.A., Grange M.L. and Pidgeon R.T. (2010) Distribution of rare earth elements in lunar zircon. *Amer. Mineral.* **95**, 273-283.

Norman M.D., Taylor G.L, Spudis P. and Ryder G. (1993) Lithologies contributing to the clast population in Apollo 17 LKFM basaltic impact melts. *In* **Workshop on Geology of the Apollo 17 Landing site**. Lunar Planetary Institute, Houston Tech. Rpt. 92-09. 42-44.

Norman M.D., Bennett V.C. and Ryder G. (2002) Targeting the impactors: highly siderophile element signatures of lunar impact melts from Serenitatis. *Earth Planet. Sci. Lett.* **202**, 217-228.

O'Kelley G.D., Eldridge J.S. and Northcutt K.J. (1974a) Cosmogenic radionuclides in samples from Taurus-Littrow: Effects of the solar flare of August 1972. *Proc. 5th Lunar Sci. Conf.* 2139-2147.

Onorato P.I.K., Uhlmann D.R. and Simonds C.H. (1976) Heat flow in impact melts: Apollo 17 Station 6 Boulder and some applications to other breccias and xenolith laden melts. *Proc. 7th Lunar Sci. Conf.* 2449-2467.

Palme H. (1980) The meteoritic contamination of terrestrial and lunar impact melts and the problem of indigenous siderophiles in the lunar highlands. *Proc. 11th Lunar Sci. Conf.* 481-506.

Phinney W.C. (1981) Guidebook for the Boulders at Station 6, Apollo 17. Curatorial Branch Publication 55, JSC- 17243 pp. 125.

Pidgeon R.T., Nemchin A.A. and Meyer C. (2006) Complex histories of two lunar zircons as evidenced by their internal structures and U-Pb ages (abs#1548). *Lunar Planet. Sci.* **XXXVII** Lunar Planetary Institute, Houston.

Rancitelli L.A., Perkins R.W., Felix W.D. and Wogman N.A. (1974a) Solar flare and lunar surface process characterization at the Apollo 17 site. *Proc. 5th Lunar Sci. Conf.* 2185-2203.

Simonds C.H. (1975) Thermal regimes in impact melts and the petrology of the Apollo 17 Station 6 boulder. *Proc. 6th Lunar Sci. Conf.* 641-672.

Wolfe E.W., Bailey N.G., Lucchitta B.K., Muehlberger W.R., Scott D.H., Sutton R.L and Wilshire H.G. (1981) The geologic investigation of the Taurus-Littrow Valley: Apollo 17 Landing Site. US Geol. Survey Prof. Paper, 1080, pp. 280.